Original Article

Partial Gene Deletion of Heart-Type Fatty Acid–Binding Protein Limits the Severity of Dietary-Induced Insulin Resistance

Jane Shearer,[1,2] Patrick T. Fueger,[1,2] Deanna P. Bracy,[1,2] David H. Wasserman,[1,2] and Jeffrey N. Rottman[2,3]

The aim of this study was to determine the contribution of heart-type fatty acid–binding protein (H-FABP) to glucose and long-chain fatty acid (LCFA) utilization in dietary-induced insulin resistance. We tested the hypothesis that H-FABP facilitates increases in LCFA flux present in glucose-intolerant states and that a partial reduction in the amount of this protein would compensate for all or part of the impairment. Transgenic H-FABP heterozygotes (HET) and wild-type (WT) littermates were studied following chow diet (CHD) or high-fat diet (HFD) for 12 weeks. Catheters were surgically implanted in the carotid artery and jugular vein for sampling and infusions, respectively. Following 5 days of recovery, mice received either a saline infusion or underwent a euglycemic insulin clamp (4 mU · kg^{-1} · min^{-1}) for 120 min. At 90 min, a bolus of 2-deoxyglucose and [^{125}I]-15-(ρ-iodophenyl)-3-R,S-methylpentadecanoic acid were administered to obtain indexes of glucose and LCFA utilization. At 120 min, skeletal muscles were excised for tracer determination. All HFD mice were obese and hyperinsulinemic; however, only HFD-WT mice were hyperglycemic. Glucose infusion rates during insulin clamps were 49 ± 4, 59 ± 4, 16 ± 4, and 33 ± 4 mg · kg^{-1} · min^{-1} for CHD-WT, CHD-HET, HFD-WT, and HFD-HET mice, respectively, showing that HET limited the severity of whole-body insulin resistance with HFD. Insulin-stimulated muscle glucose utilization was attenuated in HFD-WT but unaffected in HFD-HET mice. Conversely, rates of LCFA clearance were increased with HFD feeding in HFD-WT but not in HFD-HET mice. In conclusion, a partial reduction in H-FABP protein normalizes fasting glucose levels and improves whole-body insulin sensitivity in HFD-fed mice despite obesity. *Diabetes* 54:3133–3139, 2005

From the [1]Department of Molecular Physiology and Biophysics, Vanderbilt University School of Medicine, Nashville, Tennessee; the [2]Mouse Metabolic Phenotyping Center, Vanderbilt University School of Medicine, Nashville, Tennessee; and the [3]Department of Medicine, Vanderbilt University School of Medicine, Nashville, Tennessee.

Address correspondence and reprint requests to Jane Shearer, PhD, Director, Centre for Mouse Genomics, Faculty of Medicine, University of Calgary, Rm. 2502, 3330 Hospital Dr. NW, Calgary T2N 4N1, Canada. E-mail: jshearer@ucalgary.ca.

Received for publication 18 April 2005 and accepted in revised form 28 July 2005.

CHD, chow diet; H-FABP, heart-type fatty acid–binding protein; [^{3}H]DG, 2-deoxy[^{3}H]glucose; GIR, glucose infusion rate; HFD, high-fat diet; [^{125}I]BMIPP, [^{125}I]-15-(ρ-iodophenyl)-3-R,S-methylpentadecanoic acid; LCFA, long-chain fatty acid; NEFA, nonesterified fatty acid.

Insulin resistance is a significant risk factor in the development of numerous metabolic disease states including cardiovascular disease, diabetes, obesity, and hypertension (1,2). Due to its large mass in the body, skeletal muscle is a predominant site of insulin-stimulated glucose disposal and as such is a key site of insulin resistance. Insulin-resistant skeletal muscle is characterized by elevated rates of long-chain fatty acid (LCFA) utilization and storage, both of which contribute to impaired insulin signaling (3). As such, diminishing skeletal muscle lipid flux in skeletal muscle has emerged as a strategy for treating insulin resistance (4).

Heart-type fatty acid–binding protein (H-FABP) facilitates LCFA uptake and utilization in both skeletal and cardiac muscle. It is abundantly expressed and functions to increase LCFA solubility, facilitate diffusion, and protect against LCFA toxicity (5,6). Recent studies demonstrate that in the heart, H-FABP is essential to the partitioning of LCFA toward the mitochondria for β-oxidation or esterification (6). In this capacity, H-FABP may play a role in switching substrate utilization from glucose to LCFA in times of varied substrate supply, allowing for metabolic flexibility. Complete gene ablation (−/−) of H-FABP is known to protect against insulin resistance in isolated skeletal muscle of high-fat diet (HFD)-fed mice (7). However, these findings are difficult to extrapolate to human insulin resistance because complete genetic H-FABP deficiencies have not been reported. In humans, levels of H-FABP vary in response to numerous physiological and pathological states associated with altered rates of LCFA flux, including chronic exercise training (8), diets supplemented with (ω-3) polyunsaturated LCFA (9), and weight loss (10). These studies clearly show levels of H-FABP to be dynamic and to fluctuate with LCFA demands.

In the present study, the effects of a reduction in H-FABP levels on the development of dietary-induced insulin resistance were examined. It was hypothesized that H-FABP facilitates increases in skeletal muscle LCFA flux and that a reduction in protein level accomplished by a heterozygous germline deletion would preserve glucose utilization in insulin resistance. Under basal chow diet (CHD)-fed conditions, it was expected that the effects of reduced H-FABP would be minimal. However, when metabolically challenged with HFD feeding, a distinct phenotype would emerge. This work is central to understanding the role of H-FABP in mediating insulin resistance and the effects of reduced protein levels on substrate flux, an

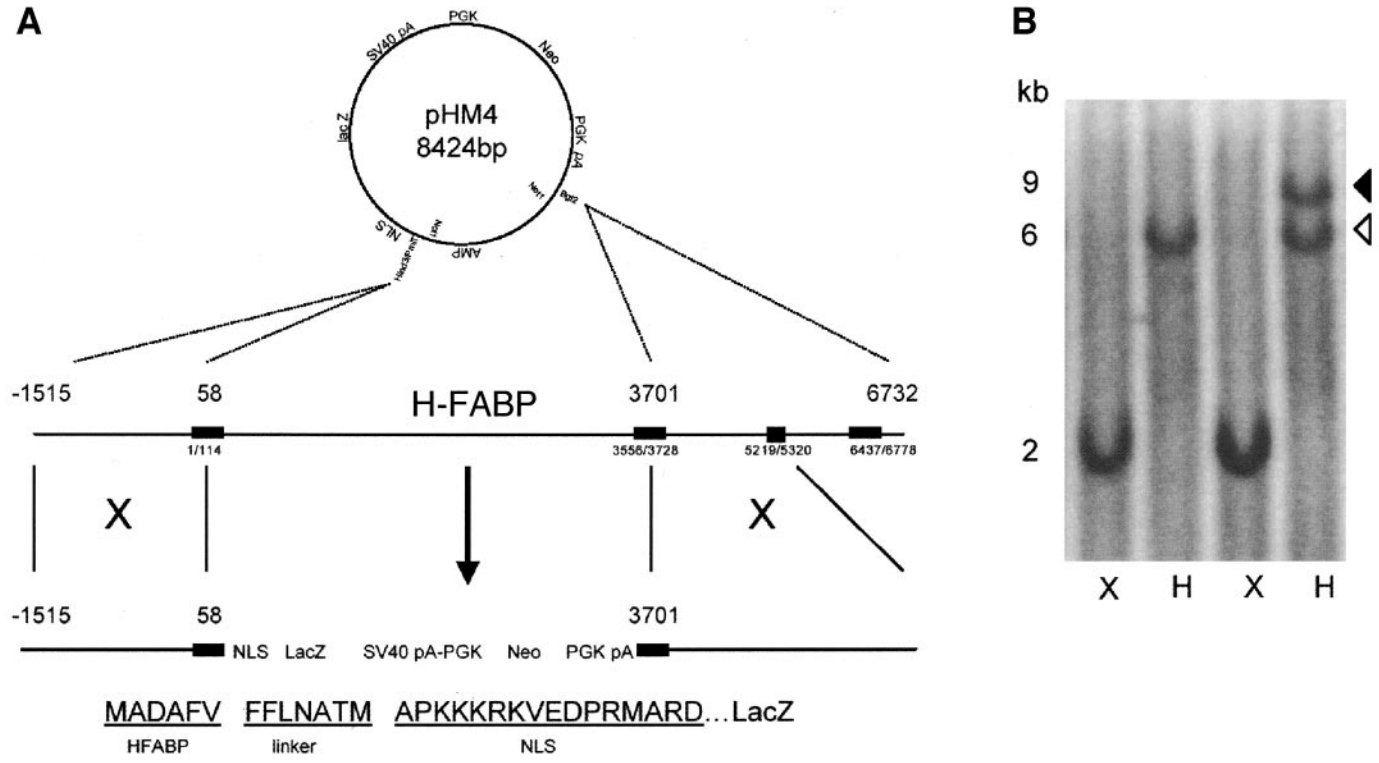

FIG. 1. Generation and phenotyping of H-FABP mice. *A*: Genomic map of H-FABP locus. *B*: Genomic Southern blot demonstrating the rearrangement in the H-FABP locus. Genomic DNA was probed with a 5′ flanking sequence contained within a 2-kb X ba1 fragment not extending into the transgene. The rearranged locus shows a 6-kb (open arrow head) to 9-kb (closed arrow head) shift in a *Hind*III (H) fragment extending into the transgene.

important consideration in the examination of H-FABP as a pharmacological target for type 2 diabetes.

RESEARCH DESIGN AND METHODS

Generation of H-FABP mice. Homologous recombination was used to replace the first two exons of the H-FABP locus with an in-frame lac-Z with a nuclear localization that signals the remaining exons lacked any initiation sites. Recombination was confirmed by Southern blotting using a 500-bp probe 2 kb 5′ of the recombination fragment, with recombination resulting in a shift of the identified EcoR1 restriction fragment from 6 to 9 kb (Fig. 1). H-FABP mice were generated by transfecting 129/SvEv embryonic stem cells. Positive clones were injected into blastocysts that were then transferred to pseudopregnant female mice. Male offspring were mated with C57BL/6J females. The resulting heterozygotes (HETs) were bred for 10 generations with C57BL/6J mice. HET and wild-type (WT) littermates were used for experiments. Details of mouse generation and genotyping results of WT and HET mice are shown in Fig. 1.

Mouse maintenance and genotyping. All procedures performed were approved by the Vanderbilt University Animal Care and Use Committee. Mice lacking H-FABP were originally produced on a 129/Balb/c background and backcrossed for at least 10 generations to C57BL/6J. Mice carrying the H-FABP transgene were subsequently bred, and following a 3-week weaning period, littermates were separated by sex, maintained in microisolator cages, and fed either a CHD or an HFD ad libitum. The caloric profile of the HFD was 16% protein, 60% fat, and 24% carbohydrate (Custom Diet F3282; Bio-Serv, Frenchtown, NJ). Mice were studied at ~4 months of age. Genotyping for the H-FABP transgene was performed on genomic DNA obtained from a tail biopsy with the PCR using 5′ GATCTCCTGTCATCTCACCTTGCTCCT 3′ (forward) and 5′ AAGAACTCGTCAAGAAGGCGATAGAAGGC 3′ (reverse) primers.

Surgical procedures. The surgical procedures were the same as those previously described (11,12). Mice were anesthetized with pentobarbitol (70 mg/kg body wt). The left common carotid artery and right jugular vein were catheterized for sampling and infusions, respectively. Lines were flushed daily with ~20 μl saline containing 200 units/ml heparin and 5 mg/ml ampicillin. Animals were individually housed after surgery, and body weight was recorded daily.

Isotopic analogues. Glucose and LCFA tracers used in the present study were 2-deoxy[^{3}H]glucose ([^{3}H]DG) and [^{125}I]-15-(ρ-iodophenyl)-3-R,S-methylpentadecanoic acid ([^{125}I]BMIPP). [^{3}H]DG was purchased from New England Nuclear (Boston, MA). [^{125}I]BMIPP was a kind gift from Dr. Russ Knapp, Oak Ridge International Laboratories (Oak Ridge, TN). Radioiodination was performed according to the manufacturer's suggested protocol. Briefly, [^{125}I]BMIPP was heated in the presence of Na^{125}I solution (740 MBq/200 μl), propionic acid, and copper (II) sulfate. $Na_2S_2O_3$ was then added and the organic phase ether extracted and sequentially back extracted with saturated $NaHCO_3$ and water. After evaporation, the [^{125}I]BMIPP was solubilized for infusion using sonication into ursodeoxycholic acid.

Experimental procedures. Experiments were performed as previously described (13) and were conducted following a postoperative recovery period of ~5 days. The recovery period was a sufficient time for body weight to be restored within 10% of presurgery body weight. On the day of the study, conscious, unrestrained mice were placed in an ~1-liter plastic container lined with bedding and fasted for 5 h ~1 h before an experiment; Micro-Renathane (0.033 OD) tubing was connected to the catheter leads and infusion syringes. Following this, a baseline ($t = -90$ min) arterial blood sample (150 μl) was drawn for the measurement of arterial blood glucose, hematocrit, and plasma insulin and nonesterified fatty acid (NEFA). The remaining erythrocytes were washed with 0.9% heparinized saline and reinfused. Mice were then infused with saline alone ($n = 30$) or with insulin (4 mU · kg^{-1} · min^{-1}) ($n = 30$). To maintain glycemia during insulin experiments, arterial blood glucose (~5 μl; HemoCue, Mission Viejo, CA) was measured at ~10-min intervals and glucose (50%) administered into the venous catheter. Mice also received saline-washed erythrocytes from a donor mouse as needed in order to maintain hematocrit within 5% of incoming hematocrit. Following a 90-min equilibration period ($t = 0$ min), an arterial blood sample (150 μl) was obtained and processed as the baseline blood sample. At $t = 5$ min, a bolus of [2-^{3}H]DG and [^{125}I]BMIPP was administered to obtain indexes of glucose and LCFA uptake and clearance. At $t = 7$, 10, 15, and 20 min, arterial blood (~50 μl) was sampled in order to determine blood glucose, plasma [2-^{3}H]DG, and [^{125}I]BMIPP. At $t = 30$ min, a final arterial blood sample was obtained (150 μl) and processed as the baseline blood sample with the addition of the determination of plasma [2-^{3}H]DG and [^{125}I]BMIPP. Mice were then anesthetized and skeletal muscles (soleus, gastrocnemius, and superficial vastus lateralis) excised and rapidly freeze clamped in liquid nitrogen. The muscle

fiber compositions of the individual skeletal muscles have been previously characterized: soleus (~44% type I, ~51% type IIA, and ~5% type IID fibers), gastrocnemius (~6% type IIA, ~11% type IID, and ~83% type IIB fibers), and superficial vastus lateralis (~3% type IIA, ~10 type IID, and 87% type IIB fibers) muscles (14). All muscle samples were subsequently stored at −80°C until further analysis.

Analytical procedures. Total H-FABP protein content was determined on gastrocnemius muscles homogenized in M-PER lysis buffer (Pierce, Rockford, IL) supplemented with protease (Pierce) and phosphatase (Sigma) inhibitor cocktails. After centrifugation (30 min at 4,500*g*), pellets were discarded and supernatants retained for protein determination using a BCA protein assay kit (Pierce). Proteins (20 μg) were separated on a 4–12% Bis-Tris SDS-PAGE gel (Invitrogen) and then transferred to a polyvinylidine fluoride membrane. Membranes were blocked, probed with rabbit H-FABP (1:3,000), and then incubated with rabbit horseradish peroxidase (1:20,000; Pierce, Rockford, IL). The membranes were then exposed to chemiluminescent substrate and images taken using the VersaDoc imaging system (Bio-Rad). To confirm equal protein loading and transfer, membranes were stripped and reprobed with monoclonal glyceraldehyde-3-phosphate dehydrogenase (1:4,000; Abcam) and then incubated with mouse horseradish peroxidase (1:20,000, Amersham). Densitometry was performed using ImageJ software (National Institutes of Health).

Immunoreactive insulin was assayed with a double-antibody method (15). NEFAs were measured spectrophotometrically (Wako NEFA C kit; Wako Chemicals, Richmond, VA). [^{125}I]BMIPP and [^{3}H]DG were measured in the same plasma (15 μl) and tissues as previously described (16). Briefly, plasma was counted for [^{125}I]BMIPP using a Beckman Gamma 5500 counter (Beckman Instruments, Fullerton, CA). Following this, the plasma sample was deproteinized in 100 μl $Ba(OH)_2$ and 100 μl $ZnSO_4$ and subsequently centrifuged. Supernatant (100 μl) was then diluted in 900 μl H_2O. ^{3}H radioactivity was counted after addition of fluor (10 ml Ultimate Gold; Packard Bioscience, Boston, MA.) using a Packard Tri-Carb 2900TR Liquid Scintillation Analyzer (PerkinElmer, Boston, MA). Similarly, ^{125}I radioactivity was determined in tissues before they were homogenized in 2 ml 0.5% perchloric acid and centrifuged for 20 min. Supernatants (1.5 ml) were then neutralized using 5M KOH and 250 μl determined by liquid scintillation counting (Packard TRI-CARB 2900TR; Packard, Meriden, CT) with Ultima Gold (Packard) as scintillant. The relationship between γ-radioactivity and β-emissions has been established in the specific counter used to measure radioactivity in these experiments (16).

Calculations. Glucose clearance (K_g) and metabolic (R_g) indexes were calculated from the accumulation of [^{3}H]DG phosphate ([^{3}H]DGP) and the integral of the plasma [^{3}H]DG concentration following a [^{3}H]DG bolus (17,18). The relationships are defined as:

$$K_g = ([^3\text{H}]\text{DGP})_m(t) / \int_0^t ([^3\text{H}]\text{DG})_p dt$$

$$R_g = K_g \times [\text{G}]_p$$

The subscripts "p" and "m" refer to mean arterial plasma and total muscle accumulation, respectively. The time interval used in the calculations was from $t = 7$ to 30 min. The measurement of R_g has been described earlier (18). In an analogous manner, LCFA clearance (K_f) and metabolic (R_f) indexes were calculated from the accumulation of [^{125}I]BMIPP in muscle and the integral of the plasma [^{125}I]BMIPP concentration following the tracer bolus.

$$K_f = ([^{125}\text{I}]\text{BMIPP})_m(t) / \int_0^t ([^{125}\text{I}]\text{BMIPP})_p dt$$

$$R_f = K_g \times (\text{FA})_p$$

where $([^{125}\text{I}]\text{BMIPP})_m$ is the [^{125}I]BMIPP in the cell and $([^{125}\text{I}]\text{BMIPP})_p$ is the [^{125}I]BMIPP present in the plasma. The measurement of R_f and K_f have been described earlier (16,19).

Statistical analyses. A two-way ANOVA was performed to detect statistical differences ($P < 0.05$). Differences within the ANOVA were determined using Tukey's post hoc test. All data are reported as means ± SE.

RESULTS

Baseline characteristics. Mouse characteristics are reported in Table 1. A total of 30 male and 30 female mice distributed between treatment groups were examined. As no effect of sex was observed (data not shown), data from male and female mice within a treatment group are considered together. Total body mass of HFD-fed mice was greater than in CHD-fed mice regardless of genotype. Despite the presence of hyperinsulinemia in both HFD-WT and HFD-HET mice, only HFD-WT were hyperglycemic. Basal NEFAs were also elevated in HFD-WT compared with CHD-WT mice. There was a tendency ($P = 0.075$) for elevated NEFA in CHD-HET compared with CHD-WT mice. Western blotting of the gastrocnemius muscle for H-FABP demonstrated HETs to have a reduction in the protein compared with WT in both CHD and HFD treatments (Fig. 2).

TABLE 1
Baseline characteristics of WT and HET H-FABP mice

	CHD		HFD	
H-FABP	WT	HET	WT	HET
Sex (M/F)	15 (7/8)	15 (7/8)	16 (8/8)	14 (8/6)
Weight (g)	26 ± 2	26 ± 2	40 ± 2*	39 ± 2*
Glucose (mmol/l)	8.53 ± 0.32	8.69 ± 0.13	10.58 ± 0.48*†	8.29 ± 0.39
NEFA (mmol/l)	1.31 ± 0.14	1.68 ± 0.14	1.84 ± 0.13*	1.59 ± 0.15
Insulin (IU/ml)	21 ± 10	19 ± 10	68 ± 10*	71 ± 10*

Data are means ± SE. *$P < 0.05$ for HFD vs. CHD within a genotype; †$P < 0.05$ for WT vs. HET within a diet.

Plasma insulin. Plasma insulin values remained unchanged with saline treatment for both genotypes within the CHD and HFD groups. During clamps, insulin infusion resulted in elevated plasma insulin levels at both 0 and 30 min in all groups. Mean insulin values at 30 min for CHD-WT and CHD-HET mice were 60 ± 10 and 50 ± 9 μU/ml, while the equivalent values for HFD-WT and HFD-HET mice were 119 ± 34 and 118 ± 19 μU/ml, respectively. HFD values were greater compared with the equivalent genotype in the CHD-fed condition.

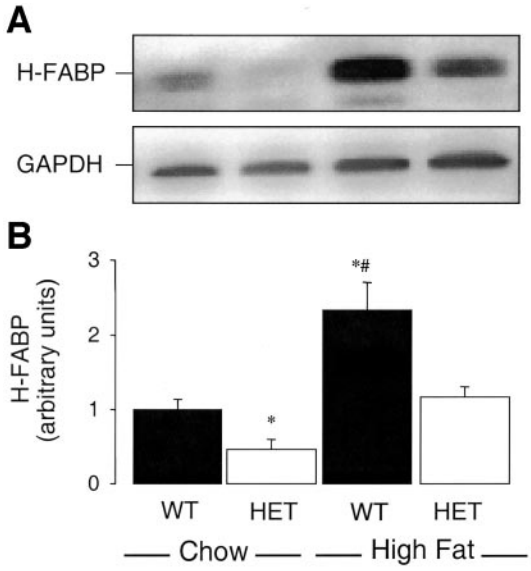

FIG. 2. Total H-FABP content in the gastrocnemius muscle in WT and HET fed either a CHD or an HFD (60% of kcal from lipid) for 12 weeks. *A*: Immunoblotting was performed to measure total H-FABP protein content. H-FABP levels were normalized to GADPH content. *B*: H-FABP content as determined by immunoblotting. Densitometry data are means ± SE. *$P < 0.05$ between WT and HET within a diet. #$P < 0.05$ from all other treatments.

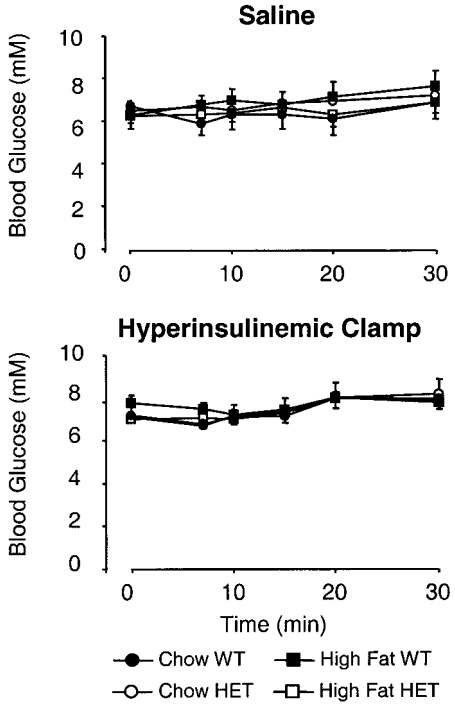

FIG. 3. Arterial blood glucose concentrations during the experimental period for saline (n = 29 total, n = 7–8 mice/group) and hyperinsulinemic treatments (n = 31 total, n = 7–8 mice/group). Mice receiving insulin were clamped at levels seen in saline-infused mice. CHD mice are indicated by circle symbols, while HFD mice are represented by square symbols. Symbols for the WT mice are filled, while those for HET H-FABP mice are open. All data are reported as means ± SE.

Arterial blood glucose and plasma NEFA. Arterial blood glucose levels for both the saline and insulin experiments are reported in Fig. 3. In the insulin-treated animals, blood glucose was clamped at levels seen with saline infusion. Plasma NEFA levels were not altered by the infusion of saline (data not shown). Infusion of insulin resulted in a suppression of NEFA from baseline values in CHD-WT and CHD-HET mice with values of 0.62 ± 0.12 and 0.59 ± 0.07 mmol/l at 30 min ($P < 0.05$, compared with Table 1). In HFD mice, 30-min NEFA values tended to but were not significantly lower than initial values with 1.05 ± 0.33 mmol/l for HFD-WT ($P = 0.064$) and 1.17 ± 0.19 mmol/l for HFD-HET ($P = 0.071$, compared with Table 1) mice.

Mean glucose infusion rates. No exogenous glucose was required in mice treated with saline (data not shown). Glucose infusion rates (GIRs) required to maintain glycemia in insulin-infused groups are shown in Fig. 4. Results demonstrate that HFD-fed mice required less glucose to maintain glycemia regardless of genotype. For WT, HFD reduced GIR by 69 and 47% in WT and HET mice, respectively, compared with CHD-fed mice despite higher circulating insulin. Within HFD, HFD-WT mice were more insulin resistant than HFD-HET mice, exhibiting a 50% reduction in GIR.

Metabolic indexes of tissue glucose utilization and clearance. R_g for saline-infused mice is shown in Fig. 5. Basal R_g was not different between genotypes in both CHD and HFD mice. Results of the insulin clamp showed no differences in R_g between CHD-WT and CHD-HET mice in all skeletal muscles studied. In contrast, HFD feeding resulted in a suppression of insulin-stimulated R_g in the soleus and vastus lateralis in HFD-WT mice, but not in

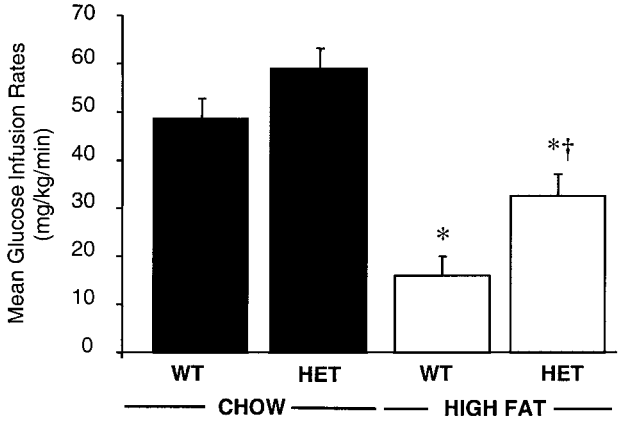

FIG. 4. Mean GIRs during insulin treatments. HET and WT H-FABP are shown. *$P < 0.05$ for HFD vs. CHD within a genotype; †$P < 0.05$ for WT vs. HET within a diet. All data are reported as means ± SE, n = 31 total, n = 7–8 mice/group.

HFD-HET mice. Within the HFD group, R_g was greater in HFD-HET mice in all muscles examined compared with that of HFD-WT mice. Results of K_g for animals undergoing the clamp protocol are shown in Fig. 7. As arterial glucose concentrations were similar in all animals, these values show the same trends as R_g (Fig. 3).

Metabolic indexes of tissue LCFA utilization and clearance. Results of R_f are shown in Fig. 6. There were no changes in R_f between CHD-WT and CHD-HET mice for

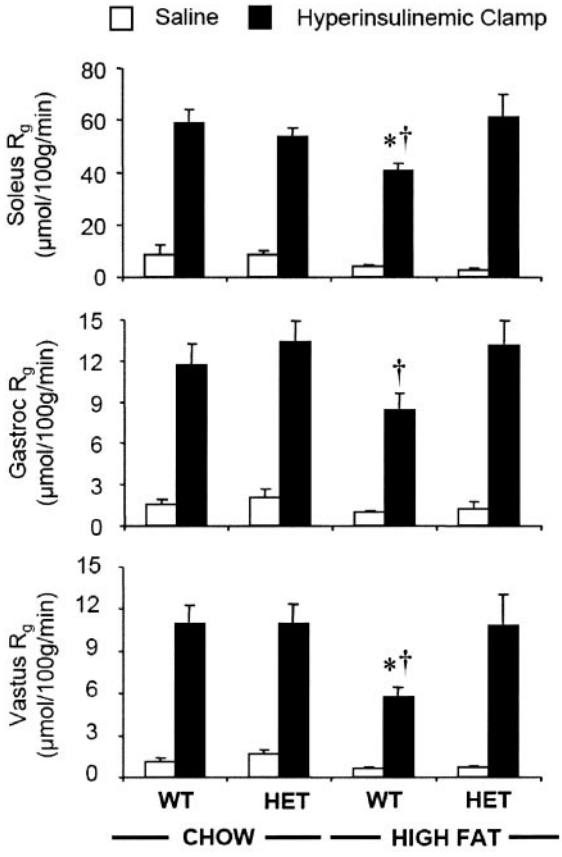

FIG. 5. Glucose utilization (R_g) in soleus, gastrocnemius (gastroc), and vastus lateralis (vastus) in saline and during the hyperinsulinemic-euglycemic clamp. □, results during saline infusion; ■, results of the insulin infusion. HET and WT H-FABP are shown. *$P < 0.05$ for HFD vs. CHD within a genotype; †$P < 0.05$ for WT vs. HET within a diet. All data are reported as means ± SE, n = 7–8 mice/group.

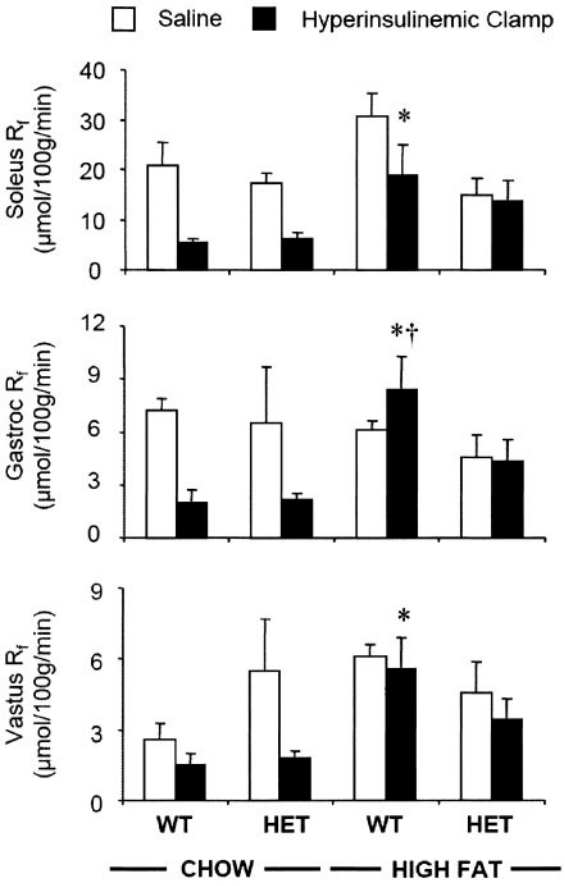

FIG. 6. Fatty acid utilization (R_f) in soleus, gastrocnemius (gastroc), and vastus lateralis (vastus) in saline and during the hyperinsulinemic-euglycemic clamp. □, results during saline infusion; ■, results of the insulin infusion. HET and WT H-FABP are shown. *$P < 0.05$ for HFD vs. CHD within a genotype; †$P < 0.05$ for WT vs. HET within a diet. All data are reported as means ± SE, n = 7–8 mice/group.

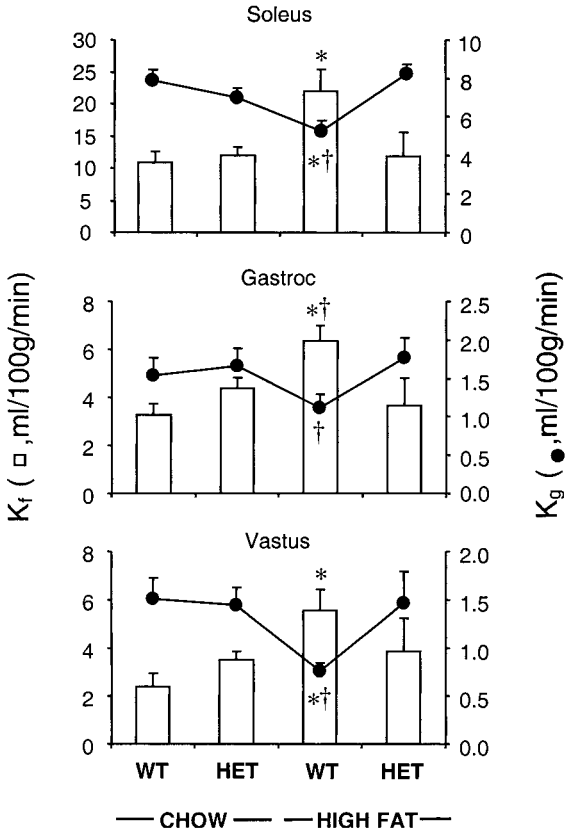

FIG. 7. Comparison of glucose (K_g) and fatty acid (K_f) clearance in individual muscles during insulin-stimulated conditions: soleus, gastrocnemius (gastroc), and vastus lateralis (vastus). Bar graphs represent K_f and are measured on the left axis, while line graphs represent K_g and are measured on the right axis. HET and WT H-FABP mice are shown. *$P < 0.05$ for HFD vs. CHD within a genotype; †$P < 0.05$ for WT vs. HET within a diet. All data are reported as means ± SE, n = 7–8 mice/group.

any muscle studied in saline-infused mice. In WT, HFD feeding resulted in elevations in R_f in the vastus lateralis with strong tendencies in the soleus muscle ($P = 0.069$). Within HFD, R_f was elevated in the soleus of HFD-WT compared with HFD-HET mice. For insulin clamps for CHD, there was no effect of genotype on R_f. Meanwhile, in HFD-WT mice, R_f was elevated in all muscles compared with CHD-WT mice. Between genotypes within HFD, R_f was elevated in HFD-WT compared with HFD-HET mice in the gastrocnemius muscle. As NEFA levels were altered with insulin infusion and R_f is a concentration-dependent measure, the results of LCFA flux are better depicted by K_f, as shown in Fig. 7.

DISCUSSION

Results of this study show dietary-induced insulin resistance to be characterized by elevated rates of LCFA flux in skeletal muscle. This augmented capacity for LCFA flux was facilitated by increases in H-FABP protein in HFD compared with CHD. These data confirm previous studies showing H-FABP levels to increase with LCFA demand and utilization such as experimental diabetes (20), exercise training (21), weight loss (10), high-fat feeding (9), and hibernation (22–24). Given the highly variable nature of H-FABP and its role in facilitating LCFA flux, the aim of the present study was to examine whether a partial genetic deletion of H-FABP was protective toward the development of dietary-induced insulin resistance.

Role of H-FABP in basal substrate utilization. Using isotopic analogues to quantify substrate flux in the conscious, unstressed mouse model, we demonstrate HET to have no impact on basal or insulin-stimulated glucose or LCFA utilization under CHD-fed conditions. This indicates that levels of H-FABP in HET are sufficient to facilitate LCFA utilization in this state. However, when metabolically challenged and made insulin-resistant by means of HFD feeding, a distinct, protective phenotype emerged. Specifically, levels of H-FABP were insufficient to meet LCFA requirements in HFD-HET mice and effectively limited LCFA flux into skeletal muscle, resulting in increased rates of both whole-body and muscle insulin-stimulated glucose utilization compared with CHD-HET mice. With CHD, HET had no impact on baseline levels of plasma glucose, insulin, or NEFA and were metabolically indistinguishable from their WT littermates with no observable differences in basal and insulin-stimulated skeletal muscle substrate utilization. These results are in agreement with previous in vitro findings of Luiken et al. (25) who show hind-limb muscle of gene-ablated H-FABP mice to have a 43% reduction in palmitate uptake in giant sacrolemmal vesicles compared with WT, yet no difference in HET muscle. This led the authors to conclude that H-FABP plays an important but merely permissive role in LCFA utilization (25). Our findings are in agreement with

this assertion as a partial reduction of H-FABP does not limit LCFA utilization under CHD-fed conditions.

Role of H-FABP in dietary-induced insulin resistance. When LCFA flux was manipulated by means of HFD feeding, a partial reduction in H-FABP was limiting to LCFA utilization. In response to a HFD, WT developed overt obesity and insulin resistance as evidenced by hyperinsulinemia, hyperglycemia, and a reduction in the amount of glucose required to maintain glycemia during the insulin clamp. Moreover, analysis of HFD-WT muscle demonstrates perturbed patterns of substrate utilization compared with that of CHD-WT. Muscle from HFD-WT displayed depressed rates of both basal R_g with a tendency toward suppression in the soleus ($P = 0.07$) and a significant decline in the vastus lateralis compared with CHD-WT. With insulin stimulation, R_g was depressed in HFD-WT versus CHD-WT in all muscles examined despite elevated levels of basal insulin in HFD. Conversely, HFD-WT increased their reliance on LCFA. This was evident in the examination of K_f, a concentration-independent measure of LCFA clearance that was increased approximately twofold in all of the muscles of HFD-WT compared with CHD-WT mice. This observation corroborates previous findings of Hegarty et al. (26) showing insulin resistance is associated with elevated tissue-specific LCFA utilization.

Like HFD-WT, HFD-HET mice became obese and hyperinsulinemic. Unlike HFD-WT, however, HFD-HET mice did not have fasting hyperglycemia. While HFD-HET displayed insulin resistance compared with CHD-fed controls, the level of glucose required to maintain glycemia was more than twofold that of HFD-WT. This indicates that while heterozygosity cannot completely prevent the development of insulin resistance, it does limit its severity. These results are consistent with and importantly extend previous findings of Erol et al. (7) who demonstrated that complete gene ablation of the H-FABP gene results in depressed palmitiate oxidation and improved skeletal muscle insulin sensitivity. Improvements in insulin sensitivity in H-FABP mice were attributed to a normalization of muscle triglyceride content that was elevated by threefold with HFD feeding (7). Given this, the mechanism by which heterozygosity reduces the severity of insulin resistance likely involves its role in facilitating LCFA oxidation and intramuscular triglyceride accumulation (27,28). In this capacity, H-FABP may have a role in directing incoming LCFA either to storage, oxidation, or esterification depending on the type of LCFA (6). When the uptake of 20:4 ω-6 and 16:0 LCFAs were examined in the hearts of H-FABP gene-ablated mice, results demonstrated that H-FABP was vital to targeting 16:0 toward β-oxidation and 20:4 ω-6 distribution to the specific phospholipid pools (6). This led the authors to conclude that H-FABP was not only an important determinant of LCFA targeting in the heart, but also to the composition of acyl chains and maintenance of phospholipid pool mass. Also of interest is an adaptation of mitochondria in gene-ablated mice. Analyses of isolated skeletal muscle mitochondria from gene-ablated mice show normal intramyofibrillar mitochondrial density but elevated numbers of subsarcolemmal mitochondria (29). According to Binas et al. (29), such an adaptation in mitochondrial density may limit the diffusion distance between cellular membranes and mitochondria, likely facilitating LCFA oxidation. Whether this adaptation occurs in HETs or clinical cases of altered H-FABP levels is not known.

H-FABP in the determination of metabolic flexibility. Results of this and previous studies clearly demonstrate that H-FABP allows muscle to switch substrates in the presence of varied substrate supply, allowing for metabolic flexibility (30). This is evident in a recent study of H-FABP mice in which exercise rather than HFD was used to perturb rates of LCFA utilization (31). During exercise, both HETs and gene-ablated mice demonstrated reductions in LCFA utilization that coincided with declining levels of the protein. Declines in LCFA utilization were matched to increases in glucose utilization, highlighting the role of this protein in mediating substrate balance. H-FABP also appears to be associated with improvements in whole-body insulin sensitivity. A study by Kempen et al. (10) demonstrated that a 12% weight loss by means of energy restriction in obese subjects was associated with a 25% increase in skeletal muscle H-FABP content. Given these improvements, the inhibition of various FABP isoforms has emerged as a pharmacological target for the treatment of type 2 diabetes. Presently, carbazole- and indole-based butanoic acid derivatives are under development for this purpose (32).

Conclusion. The present study clearly demonstrates that a partial genetic reduction in H-FABP has no impact on glucose or LCFA utilization in either basal or insulin-stimulated states under CHD-fed conditions. However, the protein is quantitatively limiting and alters patterns of substrate utilization with HFD-induced insulin resistance. In summary, we show that this genetic alteration is protective and limits the severity of dietary-induced insulin resistance. This study also highlights the value of assessing heterozygous murine models under varied conditions to uncover the physiological and pathophysiological roles of key proteins involved in the development and progression of insulin resistance.

ACKNOWLEDGMENTS

This work is supported by the National Sciences and Engineering Council of Canada (to J.S.) and National Institute of Diabetes and Digestive and Kidney Diseases Grants DK-54902 and U24-DK-59636.

The authors thank Dr. Jeffrey Clanton for his assistance with the preparation of BMIPP as well as Frejya James for her excellent technical assistance. Measurement of mouse insulin was performed with the help of Wanda L. Snead of the MMPC Hormone Assay Core.

REFERENCES

1. Reaven GM: The insulin resistance syndrome: definition and dietary approaches to treatment. *Annu Rev Nutr* 25:391–406, 2005
2. Reaven GM: Insulin resistance, cardiovascular disease, and the metabolic syndrome: how well do the emperor's clothes fit? *Diabetes Care* 27:1011–1012, 2004
3. Kelley D, Mandarino L: Fuel selection in human skeletal muscle in insulin resistance: a reexamination. *Diabetes* 49:677–683, 2000
4. Nandi A, Kitamura Y, Kahn CR, Accili D: Mouse models of insulin resistance. *Physiol Rev* 84:623–647, 2004
5. Stremmel W, Pohl L, Ring A, Herrmann T: A new concept of cellular uptake and intracellular trafficking of long-chain fatty acids. *Lipids* 36:981–989, 2001
6. Murphy EJ, Barcelo-Coblijn G, Binas B, Glatz JF: Heart fatty acid uptake is decreased in heart fatty acid-binding protein gene-ablated mice. *J Biol Chem* 279:34481–34488, 2004
7. Erol E, Cline GW, Kim JK, Taegtmeyer H, Binas B: Nonacute effects of H-FABP deficiency on skeletal muscle glucose uptake in vitro. *Am J Physiol Endocrinol Metab* 287:E977–E982, 2004
8. Schmitt B, Fluck M, Decombaz J, Kreis R, Boesch C, Wittwer M, Graber F, Vogt M, Howald H, Hoppeler H: Transcriptional adaptations of lipid

metabolism in tibialis anterior muscle of endurance-trained athletes. *Physiol Genomics* 15:148–157, 2003
9. Clavel S, Farout L, Briand M, Briand Y, Jouanel P: Effect of endurance training and/or fish oil supplemented diet on cytoplasmic fatty acid binding protein in rat skeletal muscles and heart. *Eur J Appl Physiol* 87:193–201, 2002
10. Kempen KP, Saris WH, Kuipers H, Glatz JF, Van Der Vusse GJ: Skeletal muscle metabolic characteristics before and after energy restriction in human obesity: fibre type, enzymatic oxidative capacity and fatty acid-binding protein content. *Eur J Clin Invest* 28:1030–1037, 1998
11. Halseth AE, Bracy DP, Wasserman DH: Limitations to basal and insulin-stimulated skeletal muscle glucose uptake in the high-fat-fed rat. *Am J Physiol Endocrinol Metab* 279:E1064–E1071, 2000
12. Fueger PT, Bracy DP, Malabanan CM, Pencek RR, Wasserman DH: Regulation of glucose uptake by the working muscle of conscious mice: distribution of control between transport and phosphorylation. *Am J Physiol Endocrinol Metab* 286:E77–E84, 2004
13. Halseth AE, Bracy DP, Wasserman DH: Overexpression of hexokinase II increases insulinand exercise-stimulated muscle glucose uptake in vivo. *Am J Physiol* 276:E70–E77, 1999
14. Allen DL, Harrison BC, Sartorius C, Byrnes WC, Leinwand LA: Mutation of the IIB myosin heavy chain gene results in muscle fiber loss and compensatory hypertrophy. *Am J Physiol Cell Physiol* 280:C637–C645, 2001
15. Morgan CR, Lazarow A: Immunoassay of pancreatic and plasma insulin following alloxan injection of rats. *Diabetes* 14:669–671, 1965
16. Rottman JN, Bracy D, Malabanan C, Yue Z, Clanton J, Wasserman DH: Contrasting effects of exercise and NOS inhibition on tissue-specific fatty acid and glucose uptake in mice. *Am J Physiol Endocrinol Metab* 283:E116–E123, 2002
17. Furler SM, Jenkins AB, Kraegen EW: Effect of insulin on [3H]deoxy-D-glucose pharmacokinetics in the rat. *Am J Physiol* 255:E806–E811, 1988
18. Kraegen EW, James DE, Jenkins AB, Chisholm DJ: Dose-response curves for in vivo insulin sensitivity in individual tissues in rats. *Am J Physiol Endocrinol Metab* 248:E353–E362, 1985
19. Coburn CT, Knapp FF Jr, Febbraio M, Beets AL, Silverstein RL, Abumrad NA: Defective uptake and utilization of long chain fatty acids in muscle and adipose tissues of CD36 knockout mice. *J Biol Chem* 275:32523–32529, 2000
20. Glatz JF, van Breda E, Keizer HA, de Jong YF, Lakey JR, Rajotte RV, Thompson A, van der Vusse GJ, Lopaschuk GD: Rat heart fatty acid-binding protein content is increased in experimental diabetes. *Biochem Biophys Res Commun* 199:639–646, 1994
21. Yuan Y, Kwong AW, Kaptein WA, Fong C, Tse M, Glatz JF, Chan C, Renneberg R: The responses of fatty acid-binding protein and creatine kinase to acute and chronic exercise in junior rowers. *Res Q Exerc Sport* 74:277–283, 2003
22. Eddy SF, Storey KB: Up-regulation of fatty acid-binding proteins during hibernation in the little brown bat, Myotis lucifugus. *Biochim Biophys Acta* 1676:63–70, 2004
23. Hittel D, Storey KB: Differential expression of adipose- and heart-type fatty acid binding proteins in hibernating ground squirrels. *Biochim Biophys Acta* 1522:238–243, 2001
24. Hittel D, Storey KB: The translation state of differentially expressed mRNAs in the hibernating 13-lined ground squirrel (Spermophilus tridecemlineatus). *Arch Biochem Biophys* 401:244–254, 2002
25. Luiken JJ, Koonen DP, Coumans WA, Pelsers MM, Binas B, Bonen A, Glatz JF: Long-chain fatty acid uptake by skeletal muscle is impaired in homozygous, but not heterozygous, heart-type-FABP null mice. *Lipids* 38:491–496, 2003
26. Hegarty BD, Cooney GJ, Kraegen EW, Furler SM: Increased efficiency of fatty acid uptake contributes to lipid accumulation in skeletal muscle of high fat-fed insulin-resistant rats. *Diabetes* 51:1477–1484, 2002
27. Kelley DE, Mokan M, Simoneau JA, Mandarino LJ: Interaction between glucose and free fatty acid metabolism in human skeletal muscle. *J Clin Invest* 92:91–98, 1993
28. Kelley DE, Goodpaster BH: Skeletal muscle triglyceride: an aspect of regional adiposity and insulin resistance. *Diabetes Care* 24:933–941, 2001
29. Binas B, Han X-X, Erol E, Luiken JJFP, Glatz JFC, Dyck DJ, Motazavi R, Adihetty PJ, Hood DA, Bonen A: A null mutation in H-FABP only partially inhibits skeletal muscle fatty acid metabolism. *Am J Physiol Endocrinol Metab* 285:E481–E489, 2003
30. Storlien L, Oakes ND, Kelley DE: Metabolic flexibility. *Proc Nutr Soc* 63:363–368, 2004
31. Shearer J, Fueger PT, Rottman JN, Bracy DP, Binas B, Wasserman DH: Heart-type fatty acid-binding protein reciprocally regulates glucose and fatty acid utilization during exercise. *Am J Physiol Endocrinol Metab* 288:E292–E297, 2005
32. Lehmann F, Haile S, Axen E, Medina C, Uppenberg J, Svensson S, Lundback T, Rondahl L, Barf T: Discovery of inhibitors of human adipocyte fatty acid-binding protein, a potential type 2 diabetes target. *Bioorg Med Chem Lett* 14:4445–4448, 2004